

Analysis of composite T beam composed of timber, concrete and carbon strip

MATJAŽ TAJNIK, PETER DOBRILA, MIROSLAV PREMROV

Faculty of civil engineering

University of Maribor

Smetanova ulica 17, SI – 2000 Maribor

SLOVENIA

matjaz.tajnik@uni-mb.si <http://www.fg.uni-mb.si>

Abstract: This paper provides a mathematical model and numerical example of composite T-section composed of a concrete plate and a timber beam strengthened at the bottom tension side with a carbon fibre-reinforced polymer (CFRP) strip. Analysis is provided in accordance with the European standards for timber, steel and concrete structures. The tensile strength of the carbon strip as well as the compressive strength of the concrete plate are higher than the bending strength of the timber beam, therefore it is convenient to use such composition of material to gain a higher load bearing capacity. It has been shown that the inclusion of CFRP strip reinforcement on the increase of load carrying and bending stiffness capacity was not as high as expected. On the other hand, we realized the importance of variety of material grade and geometrical properties combinations between sub-components which can significantly improve load bearing capacity and stiffness of composed beam. Furthermore, the CFRP strip contribution to the bending resistance and stiffness of the element is presented as a function of the fastener spacing intervals between concrete plate and timber beam.

Key-Words: Composite structures, Timber structures, Carbon strip, Load bearing capacity, Modelling,

1 Introduction

Nowadays, the significance of the protection and reconstruction of old and historic buildings is increasing in modern planning. Therefore, an efficient type of floor system which consists of timber members in the tensile zone, a thin concrete layer in compression zone and the connection between timber and concrete has drawn attention of the experts in the field of civil engineering. The results of such reconstruction-strengthening procedure or new composite construction (compared to timber floors) are increase of stiffness, load bearing capacity, improved sound insulation and better fire resistance.

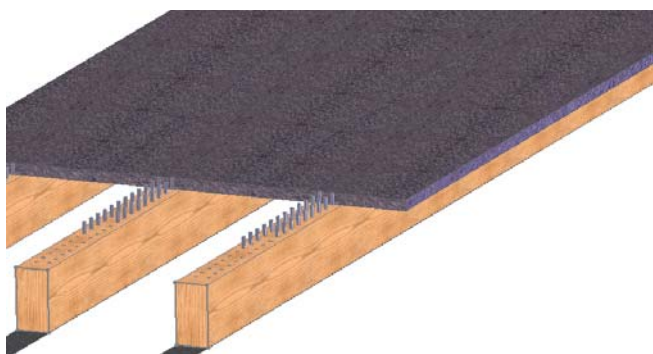


Fig. 1: Model of reconstruction of timber floor

The structural behaviour of timber-concrete composite members is governed by the shear connection between them. Whatever system of fasteners is used in composed

section, steel fibre reinforced concrete (SFRC) shows much better characteristics than classic reinforced concrete. Holschemacher, Klotz and Weibe (2002) demonstrated their experimental studies using SFRC [9]. That solution makes the reduction of slab thickness possible, under flexure the initial crack load can be increased. When the first crack occurs the released forces can be transferred over the crack and therefore brittle failure is prevented. When applying SFRC, the experiment shows that the behaviour is more ductile and redistribution of stresses is better. Ultimate load carrying capacity of fastener is 27% higher and initial slip modulus is 180% higher.

Since the tensile strength of timber is usually not much lower than the compressive strength, the applications of fibre reinforced polymers (FRP) or carbon fibre reinforced polymers (CFRP) in timber have not been as frequently used as in masonry or especially in concrete structures. The potential of FRP in combination with steel and timber structures has only been explored recently. The main advantages of using FRP in particular compared to other materials (for example steel plates) are their corrosion resistance, light weight and flexibility, which allow convenient and easy transport to the place of erection.

The availability of advanced composite materials has stimulated much interest in reinforcement of timber elements, especially on glued laminated beams. Timber is an uncommon material for critical highway bridge structures, though several applications of strengthening

using FRP and CFRP to gain higher ductility and bending resistance can be found in this field. Dagher and Breton (1998) researched reinforced laminated timber beams in the tensile area using FRP lamellas. The test results showed an essential increase in bending resistance. Stevens and Criner (2000) conducted an economic analysis of FRP gluelam beams. The results showed practical applicability of FRP reinforced elements, especially for bridges of greater spans, where beam dimensions can be substantially reduced using the presented FRP solution. The test results using carbon fibres in laminated beams are presented in Bergmeister and Luggin (2001).

Composite reinforcement on sawn timber elements is less common in literature although many applications exist, especially for retrofitted reinforcement. Timber beams reinforced by a layer of high-modulus composite material may be analysed using a transformed section of an equivalent wood (Johns and Lacroix, 2000), but the influence of composite reinforcement on the bending resistance of the timber elements is usually not particularly high. Unlike concrete or masonry, the contribution of the timber tension zones to the bending resistance continues to be very high. Johns and Racine (2001) demonstrated their experimental studies using glass fibres to reinforce sawn timber sections. The test results presented there show that strength increase is far greater than those predicted by simple engineering bending calculations. They confirm that the composite material adjacent to the sawn wood, even wood of low quality, has an essential effect on the wood elements. Studies of the wood members reinforced with FRP materials in the form of sheets (Triantafillou, 1997) also show that the effectiveness of FRP reinforcement can be quite high, and that is maximized when the fibres are placed in the longitudinal direction of elements.

Use of HSF and CFRP for the reconstruction and strengthening of timber elements opens new perspectives for timber structures design. Continuously decreasing prices of these materials make the new technology more economical and interesting. On the other hand, applying composite fibres to timber structures requires experience and higher quality of workmanship than traditional reinforcements.

2 Analytic solution for derivation of load carrying capacity and stiffness

For design purposes, a simplified design method for mechanically jointed elements according to Annex B of Eurocode 5 [3] is used. Expression of the so called » γ -method« is used in equations with the following fundamental assumptions [4, 5]:

- Bernoulli's hypothesis is valid for each sub-component,
- material behaviour of all sub-components is linear elastic,
- the distances between the dowels are constant along the beam,
- slip modulus is taken in plastic area for ultimate limit state and elastic area for serviceability limit state (Fig.2),
- bending moment varying sinusoidally or parabolically.

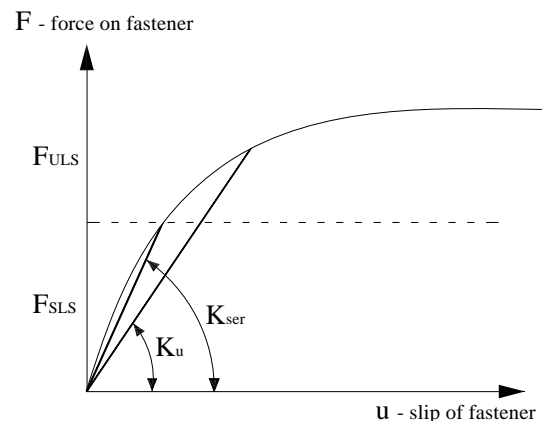


Fig. 2: F-u diagram for slip in the connection

Basic determinations

Equation (1) shows the position of the neutral axis of the composed section which is analogous to Eurocode 5 [3] for mechanically jointed elements:

$$z_t = \frac{\sum S_{y,i}^{\gamma_{ct}}}{\sum A_i} = \frac{(n_f \cdot A_f \cdot (h_t + h_f) - n_c \cdot \gamma_{ct} \cdot A_c \cdot (h_t + h_c))}{2 \cdot (n_c \cdot \gamma_{ct} \cdot A_c + A_t + n_f \cdot A_f)} \quad (1)$$

where z_t is position of overall neutral axis from centre of gravity of timber member, n_i is given by equation (2), γ_{ct} is stiffness coefficient given by equation (3), A_i is area of subcomponent shown on Fig.2 and h_i is thickness of each sub component shown on Fig.3.

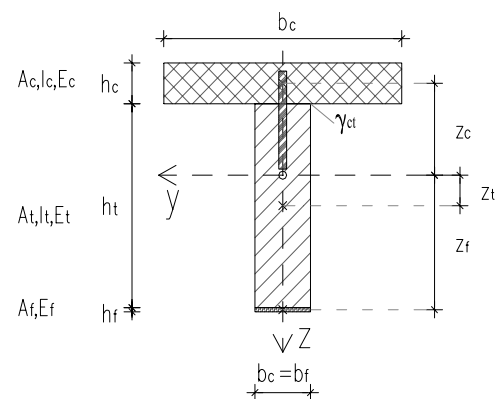


Fig. 3: Composite cross-section

Relations between modulus of elasticity are:

$$n_c = \frac{E_c}{E_t} \text{ for concrete; and } n_f = \frac{E_f}{E_t} \text{ for CFRP} \quad (2)$$

where E_c is mean modulus of elasticity of concrete, E_t is mean modulus of elasticity of timber and E_f is mean modulus of elasticity of carbon strip (fibre).

Distances from centre of gravity of each sub-component to main neutral axe can be obtained as written below:

$$z_c = \left(-\frac{h_t}{2} - z_t \right) - \frac{h_c}{2} \quad \text{for concrete slab} \quad (3)$$

$$z_f = \left(\frac{h_t}{2} - z_t \right) + \frac{h_f}{2} \quad \text{for carbon strip} \quad (4)$$

where z_i is distance from overall neutral axe to centre of gravity of each subcomponent.

In upper forms the stiffness coefficient of the fasteners in plane between concrete and timber (γ_{ct}) can be defined using Eurocode 5 [3] in the form of:

$$\gamma_{ct} = \frac{1}{1+k}; \quad k = \frac{\pi^2 \cdot E_{cm} \cdot A_c \cdot s_i}{K \cdot l_{eff}^2} \quad (5)$$

where l_{eff} is effective (buckling) length of composed beam, A_c is effective area of concrete plate, s_i is effective spacing between the fastener and K is slip modulus taken from Eurocode 5 [3] for dowel type of fasteners where for concrete to timber connections K_{ser} (slip modulus for serviceability) should be based on mean density (ρ_m) of timber member and finally be increased (multiplied) by 2,0. The stiffness coefficient in plane between carbon strip and timber which are glued together is considered as fully connected ($\gamma_f = 1.0$). So the final form for K is:

$$K_{ser} = 2.0 \cdot \frac{\rho_m^{1.5} \cdot d}{23} \quad \text{for serviceability limit state} \quad (6)$$

$$K_u = \frac{2}{3} K_{ser} \quad \text{for ultimate limit state} \quad (7)$$

The effective bending stiffness $(EI_y)_{eff}$ of mechanically jointed elements taken from Eurocode 5 [3], can be analogically written in the form of:

$$(EI_y)_{eff} = E_c \cdot \left(\frac{h_c^3 \cdot b_c}{12} + \gamma_{ct} \cdot A_c \cdot z_c^2 \right) + \quad (8)$$

$$E_t \cdot \left(\frac{h_t^3 \cdot b_t}{12} + A_t \cdot z_t^2 \right) + E_f \cdot (A_f \cdot z_f^2)$$

By using relations between modulus of elasticity from equations (2) the effective bending stiffness is developed as:

$$E_t \cdot I_{y,eff} = E_t \cdot \left(n_c \cdot \left(\frac{h_c^3 \cdot b_c}{12} + \gamma_{ct} \cdot A_c \cdot z_c^2 \right) + \left(\frac{h_t^3 \cdot b_t}{12} + A_t \cdot z_t^2 \right) + n_f \cdot (A_f \cdot z_f^2) \right) \quad (9)$$

Determination of bending bearing capacity

Normal stresses in composite section for each of sub-components are defined in form of:

$$\sigma = \frac{M}{W} = \frac{M_y \cdot E_i}{(EI_y)_{ef}} \cdot (\gamma_i \cdot z_i \pm \Delta z) \quad (10)$$

where M_y is belonging bending moment around appropriate axe (Fig.2), Δz is distance from centre of gravity of each subcomponent to an edge (or any fibre) of each subcomponent, E_i modulus of elasticity for appropriate subcomponent. With usage of equation (10) and (8) normal stresses in the edges of the concrete slab (see Fig. 4) are obtained in the form of:

$$\sigma_c = \frac{M_y \cdot n_c}{I_{y,ef}} \cdot \left(\gamma_{ct} \cdot z_c \pm \frac{h_c}{2} \right) \leq f_{c,k} \quad (11)$$

where $f_{i,k}$ represent characteristic strength of sub-component material under normal stress. For normal stresses in the edge fibres of the timber beam in form of:

$$\sigma_t = \frac{M_y}{I_{y,ef}} \cdot \left(z_t \pm \frac{h_t}{2} \right) \leq f_{m,k} \quad (12)$$

For normal stresses in the centre of timber beam (Fig. 4):

$$\sigma_t = \frac{M_y}{I_{y,ef}} \cdot (z_t) \leq f_{t,0,k} \quad (13)$$

For normal stresses in the edge fibres of CFRP (Fig. 4):

$$\sigma_f = \frac{M_y \cdot n_f}{I_{y,ef}} \cdot \left(z_f \pm \frac{h_f}{2} \right) \leq f_{f,k} \quad (14)$$

According to equations from (11) to (14) design bending moment (capacity) can be evaluated:

$$M_{y,d} = \sigma_d \cdot W_{y,ef} = f_{i,d} \cdot \frac{I_{y,ef}}{n_i \cdot (\gamma_i \cdot z_i \pm \Delta z)} \quad (15)$$

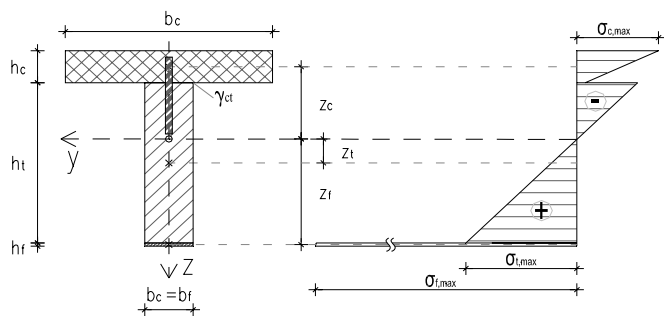


Fig. 4: Diagram of normal stress in cross-section

If concrete slab under compression is decisive equation (16) is obtained:

$$M_{y,d,c} = \frac{\alpha}{\gamma_c} \cdot M_{y,k,c} = \frac{\alpha}{\gamma_c} \cdot \left(f_{c,k} \cdot \frac{I_{y,ef}}{n_c \cdot \left(\gamma_{ct} \cdot z_c - \frac{h_c}{2} \right)} \right) \quad (16)$$

If timber beam is decisive (what is mostly the case) under bending normal stress equation (17) is obtained:

$$M_{y,d,t} = \frac{k_{mod}}{\gamma_m} \cdot M_{y,k} = \frac{k_{mod}}{\gamma_m} \cdot \left(f_{m,y,k} \cdot \frac{I_{y,ef}}{z_t + \frac{h_t}{2}} \right) \quad (17)$$

In cases when the normal stress in the centre of timber beam is high the equation (18) must be used if equation (19) is fulfilled:

$$M_{y,d,t} = \frac{k_{mod}}{\gamma_m} \cdot M_{y,k} = \frac{k_{mod}}{\gamma_m} \cdot \left(f_{t,0,k} \cdot \frac{I_{y,ef}}{z_t} \right) \quad (18)$$

$$1 + \frac{h_t}{2 \cdot z_t} > \frac{f_{m,k}}{f_{t,0,k}} \quad (19)$$

If carbon strip is decisive under tension equation (18) is obtained:

$$M_{y,d,f} = \frac{1}{\gamma_f} \cdot M_{y,k,f} = \frac{1}{\gamma_f} \cdot \left(f_{f,k} \cdot \frac{I_{y,ef}}{n_f \cdot \left(z_f + \frac{h_f}{2} \right)} \right) \quad (20)$$

Determination of shear bearing capacity

Shear stresses in section for any fibre are given as:

$$\tau = \frac{V \cdot S}{I \cdot b} = \frac{V_z \cdot \sum S_{y,i}^{(\gamma)} \cdot n_i}{I_{y,ef} \cdot b_i} \quad (21)$$

where V_z is belonging shear force in direction of appropriate axe (Fig.3), Δz is first moment of area of section above (or below) appropriate fibre in function of subcomponent modulus of elasticity and potential stiffness coefficient (γ_{ct}), b_i is belonging width of section at appropriate fibre. With usage of equation (21) shear stress in the bottom edge of concrete slab (see Fig. 5) is obtained in the form of:

$$\tau_c^{max} = \frac{V_z \cdot n_c \cdot (\gamma_{ct} \cdot (h_c \cdot b_c) \cdot |z_c|)}{I_{y,ef} \cdot b_c} \leq \tau_{R,k,1} \quad (22)$$

For determination of maximal shear stress at neutral axe of the composite cross section the equation (23) is used:

$$\tau_t^{max} = \frac{V_z \cdot \left(n_c \cdot \gamma_{ct} \cdot (h_c \cdot b_c) \cdot |z_c| + b_t \cdot \left(\frac{h_t}{2} - z_t \right) \cdot \left(\frac{h_t}{4} - \frac{z_t}{2} \right) \right)}{I_{y,ef} \cdot b_t} \leq f_{v,k} \quad (23)$$

Shear stress in upper fibres of CFRP is given as:

$$\tau_f = \frac{V_z \cdot S_{y,i}^{(\gamma)} \cdot n_i}{I_{y,ef} \cdot b_t} = \frac{V_z \cdot (n_f \cdot (h_f \cdot b_f) \cdot z_f)}{I_{y,ef} \cdot b_f} \leq \tau_{Rf,k} \quad (24)$$

where $f_{v,k}$, $\tau_{i,k}$ present characteristic shear strength of subcomponent material accordingly to Eurocode 5 [3]. For concrete plate accordingly to Eurocode 2 [4] characteristic shear strength is taken as:

$$\tau_{R,k,1} = \tau_{R,k} \cdot k \cdot (1.2 + 40 \cdot \rho_l) \quad (25)$$

Where $\tau_{R,k}$ present basic characteristic shear strength of concrete reading from Eurocode 2 (4), $k = (1.6 - d)$ where d is static height of concrete slab in meters and ρ_l is longitudinal reinforcement percentage.

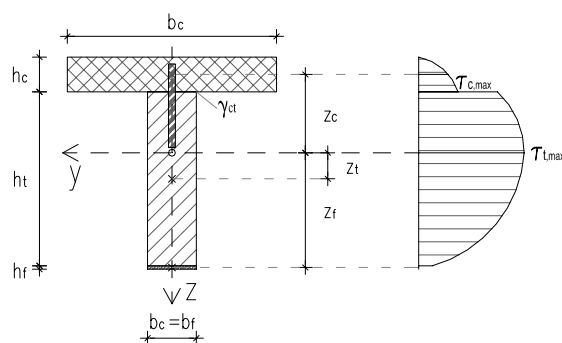


Fig. 5: Diagram of shear stress in cross-section

According to equations (22) - (24) design shear force (capacity) can be evaluated as:

$$V_{z,d,i} = f_{i,d} \cdot \frac{I_{y,ef} \cdot b_i}{\sum S_{y,i}^{(\gamma)} \cdot n_i} \quad (26)$$

If concrete slab is decisive the equation (27) is obtained:

$$V_{z,d,c} = \frac{1}{\gamma_c} \cdot V_{z,k,c} = \frac{1}{\gamma_c} \cdot \left(\tau_{R,k,1} \cdot \frac{I_{y,ef} \cdot b_c}{n_c \cdot (\gamma_{ct} \cdot (h_c \cdot b_c) \cdot |z_c|)} \right) \quad (27)$$

And if timber beam is decisive the equation (28) is obtained:

$$V_{z,d,t} = \frac{k_{mod}}{\gamma_m} \cdot V_{z,k,t} = \frac{k_{mod}}{\gamma_m} \cdot \left(f_{v,k} \cdot \frac{I_{y,ef} \cdot b_t}{n_c \cdot \gamma_{ct} \cdot (h_c \cdot b_c) \cdot |z_c| + b_t \cdot \left(\frac{h_t}{2} - z_t \right) \cdot \left(\frac{h_t}{4} - \frac{z_t}{2} \right)} \right) \quad (28)$$

It is also recommended to control shear between web and flanges according to Eurocode 2 (4).

Determination of fastener bearing capacity

Force on one fastener from equation (21) in function of distances between fasteners (s_i) is given as:

$$F_i = \frac{V_z \cdot S_i \cdot E_i}{(EI_y)_{ef}} \cdot s_i = \frac{V_z \cdot \sum S_{y,i}^{(\gamma)} \cdot n_i}{I_{y,ef}} \cdot s_i \quad (29)$$

On this point, construction parameters given by Eurocode 5 [3] must be also considered as minimum intervals, edge and end distances for different types of fasteners.

In our case, the design force on one fastener for connection between concrete slab and timber beam (see Fig. 6) is obtained in the form of:

$$F_{v,d} = \frac{V_{z,d} \cdot n_c \cdot (\gamma_{ct} \cdot (h_c \cdot b_c) \cdot |z_c|)}{I_{y,ef}} \cdot s_i \leq F_{v,Rd} \quad (30)$$

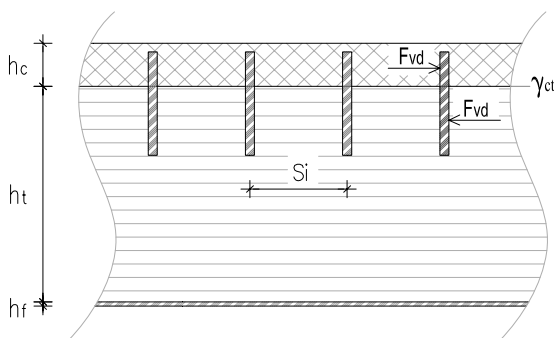


Fig. 6: Fasteners and forces on it

Consequently design shear force is given as:

$$V_{z,d} = \frac{k_{mod}}{\gamma_m} \cdot V_{z,k} = \frac{k_{mod}}{\gamma_m} \cdot \left(\frac{F_{v,Rk} \cdot I_{y,ef}}{n_c \cdot (\gamma_{ct} \cdot (h_c \cdot b_c) \cdot |z_c|) \cdot s_i} \right) \quad (31)$$

Where the competent $F_{v,Rk}$ is characteristic load carrying capacity per shear plane per fastener given in Eurocode 5 part 1-1 [3] (according to the Johansen yield theory) and modified according to Eurocode 5 part 2 [5].

The load carrying capacity of fastener can be additionally controlled according to Eurocode 4 part 1-1 [6] in spite of decisive Eurocode 5 part 1-1 [3].

2.5 Bending stiffness for serviceability limit state

In these section the determination of bending stiffness for composite section is represented, which is needed for determination of deflections and vibrations according to Eurocode 5 [3] and Eurocode 2 [4].

2.5.1 Instantaneous bending stiffness ($t = 0$)

The equations (2) - (4) remain the same, equations (1), (7) and (9) are modified by γ_{ct} where usage of K_{ser} instead of K_u makes the only difference in equation (5).

2.5.2 Final bending stiffness ($t = \infty$)

The time dependent effects (domination of creep) can be associated with the modulus of elasticity of each material of sub-component. In equations (2) the modified so called effective modulus of elasticity according to Eurocode 5 [3] and Eurocode 2 [4] are used in the form of:

$$E_{t,fin} = \frac{E_t}{1 + \Psi_2 \cdot k_{def}} \quad \text{for timber sub-section} \quad (32)$$

$$E_{c,eff} = \frac{E_c}{1 + \phi_{(\infty, t_0)}} \quad \text{for concrete sub-section} \quad (33)$$

Time dependent effects presented in connection are associated with modulus K_{ser} as modified equation from Eurocode 5 [3]:

$$K_{ser,fin} = \frac{K_{ser}}{1 + \left(\frac{\Psi_2 \cdot k_{def} + \phi_{(\infty, t_0)}}{2} \right)} \quad (34)$$

That have direct influence on (γ_{ct}) in equation (5) and consequently on equation (1) and on bending stiffness given in equations (7) – (8). There is still some uncertainty about suitable modelling time dependent effects on composition of different materials together.

However, the influence of creep in ultimate limit state (ULS) calculations must not be neglected on such kind of composed sections. The creep has big influence on rearrangement of stresses by section especially when

section is composed from different creep depended materials.

According to [11] the stresses in a concrete part of composite element cross-section decrease in time significantly (from 1.4 to 5 times) while it slightly increases in timber part (approximately 2 times). In before mentioned study, the creep effects presented in connection between timber and concrete part of section were not taken into account, although they have big influence on distribution of stress.

Also, research given by [12] shows comparison between long term service load (18kN on inclined screws and 10kN on dowels with concrete connectors) and short term (24kN on inclined screws and 25kN on dowels with concrete connectors) load respectively.

From that can be concluded that the rheological phenomena (creep) of connection in calculation of deformation - serviceability limit state and also in calculation of bearing capacity of element section - ultimate limit state must be taken into account.

In our presented study, creep effects present in connection are taken into account through final slip modulus $K_{ser,fin}$.

3 Numerical example

3.1 Geometrical and material properties

Numerical analysis is performed for composite T section of actual dimensions shown in Fig.7. For fasteners between concrete plate and timber beam we use dowels according to Eurocode 5 [3] and Eurocode 3 [8] of $\Phi 20$ mm and length $l = 24$ cm at constant intervals of $s = 10$ cm. Dowel (bolt) grade according to Eurocode 3 [2] is 8.8 ($f_{yb} = 640N/mm^2$, $f_{ub} = 800N/mm^2$).

Material properties for the timber quality GL24h are taken from EN 1194 [7], for the concrete slab from Eurocode 2 [4] and the CFRP – SikaWrap-230C from [2]. For all materials safety factors appropriate European standards are used. For FRP strengthening materials is recommended to use TR55 – Technical Report 55 (Concrete Society UK). All material properties are listed in Table 1.

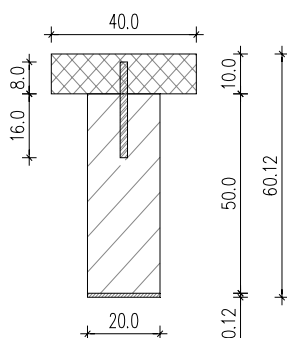


Fig. 7: Cross-section (dimension in cm).

	Concrete C30/37	Timber GL24h	SikaWrap 230C
$E_{0,m}$ [kN/cm ²]	3193.9	1160	23100
$f_{m,k}$ [kN/cm ²]	/	2.444	/
$f_{t,0,k}$ [kN/cm ²]	0.2028	1.65	410.0
$f_{c,0,k}$ [kN/cm ²]	3.0	2.4	/
ρ_k [kg/m ³]	/	380	/
ρ_m [kg/m ³]	2400	456	1833.3

Table 1: Properties of used materials

For load, 50% of permanent and 50% of long term (storage) action is predicted. On that assumption, the proper safety factors for ultimate limit state and modification factors for long term effects can be determined. The effective length of beam ($l_{eff} = 800cm$) is also predicted for determination of the stiffness coefficient γ_{ct} .

3.2 Determination of creep for timber beam

According to Eurocode 5 [3] creep coefficient for timber is calculate as:

$$\psi_2 \cdot k_{def} \quad (35)$$

where $k_{def} = 0.6$ presents the final creep coefficient for service class 1 given by Eurocode 5 [3]. The factor for quasi-permanent value of action is $\psi_2 = 0.6$ for long term action (C or D category) and $\psi_2 = 1.0$ for permanent action given by Eurocode 1.

As already mentioned, 50% of permanent and 50% of long term load were predicted so the final creep coefficient is calculated as mean value between corresponded permanent and long term value of load:

$$\psi_2 \cdot k_{def} = \frac{\psi_{2g} \cdot k_{def}}{2} + \frac{\psi_{2p} \cdot k_{def}}{2} = \frac{1.0 \cdot 0.6}{2} + \frac{0.6 \cdot 0.6}{2} = 0.48 \quad (36)$$

3.3 Determination of creep for concrete plate

According to Eurocode 2 [4] model developed by CEB Commision VIII and GTG9 (based on Rüsck model) the creep coefficient for concrete is calculated as shown further where 50% relative humidity of the ambient environment and 28 days age of concrete at loading are predicted.

Equation for creep coefficient at time "t" is given as:

$$\phi_{(\infty,t_0)} = \phi_0 \cdot \beta_c(t - t_0) \quad (37)$$

where ϕ_0 present basic (final) creep coefficient as:

$$\phi_0 = \phi_{RH} \cdot \beta(f_{cm}) \cdot \beta(t_0) = 2.16 \cdot 2.725 \cdot 0.488 = 2.872$$

where we use:

- factor of relative humidity:

$$\phi_{RH} = 1 + \frac{1 - RH}{0.1 \cdot \sqrt[3]{h_0}} = 1 + \frac{1 - 50}{0.1 \cdot \sqrt[3]{80}} = 2.16$$

with $RH = 50\%$

$$h_0 = \frac{2 \cdot A_c}{u} = \frac{2 \cdot b_c \cdot h_c}{2 \cdot b_c + 2 \cdot h_c} = \frac{2 \cdot 40 \cdot 10}{2 \cdot 40 + 2 \cdot 10} = 8.0 \text{ cm} = 80 \text{ mm}$$

- factor of concrete strength:

$$\beta(f_{cm}) = \frac{16.8}{\sqrt{f_{cm}}} = \frac{16.8}{\sqrt{38}} = 2.725$$

with $f_{cm} = f_{ck} + 8 = 38 \frac{\text{N}}{\text{mm}^2}$

- factor of concrete age at loading:

$$\beta(t_0) = \frac{1}{(0.1 + t_0^{0.2})} = 0.488$$

with $t_0 = 28 \text{ dni}$

The coefficient of time development of creep (fully developed in presented case):

$$\beta_c(t - t_0) = \left(\frac{t - t_0}{\beta_H + t - t_0} \right)^{0.3} = 1.0$$

where final creep coefficient may be adopted for concrete at 70 years:

$t = 70 \cdot 365 = 25550 \text{ days}$ and age of concrete at loading as already mentioned: $t_0 = 28 \text{ days}$

The creep coefficient at time “ $t = \infty$ ” is finally calculated and modified for mean modulus of elasticity (model is associated with tangent modulus) which is used in presented study:

$$\phi_{(\infty, t_0)} = \phi_0 \cdot \beta_c(t - t_0) \cdot \frac{E_{cm}}{E_{c(28)}} = 2.872 \cdot 1.0 \cdot \frac{1}{1.05} = 2.735 \quad (38)$$

3.4 Results of numerical analysis

	SLS $t = 0$	SLS $t = \infty$	Units	Equation
K	169.35	64.946	kN/cm	(7) / (8)
γ_{ct}	0.4622	0.2479	/	(5)
n_c	2.753	1.091	/	(2)
n_f	19.914	29.472	/	(2)
z_o	-9.040	-1.250	cm	(1)
z_c	-20.960	-28.750	cm	(3)
z_f	34.100	26.310	cm	(4)
z_t	9.040	1.250	cm	(1)
I_{y,ef}	$5.7846 \cdot 10^5$	$3.5192 \cdot 10^5$	cm ⁴	(9)
(EI)_{y,ef}	67101.18	27583.40	kNm ²	(8)

Table 2: Results of numerical analysis for SLS.

	ULS $t = 0$	ULS $t = \infty$	Units	Equation
K	112.90	43.30	kN/cm	(7) / (8)
γ_{ct}	0.3643	0.4508	/	(5)
n_c	2.753	1.09	/	(2)
n_f	19.914	29.47	/	(2)
z_o	-7.48	-3.258	cm	(1)
z_c	-22.52	-26.742	cm	(3)
z_f	32.54	28.318	cm	(4)
z_t	7.48	3.258	cm	(1)
I_{y,ef}	$5.2755 \cdot 10^5$	$4.2000 \cdot 10^5$	cm ⁴	(9)
(EI)_{y,ef}	61194.61	32918.76	kNm ²	(8)
M_{y,d,t}	222.31	203.43	kNm	(17)
V_{z,d,t}	131.79	127.16	kN	(28)
V_{z,d}	89.51	101.99	kN	(31)

Table 3: Results of numerical analysis for ULS.

Research given by [13] shows that the modulus of sliding after time period of 426 days is 62% of initial value ($K_{u(t=426)} = 0.62K_u$) for wood-concrete connection made of Type C dowels according to DIN. In comparison to presented study from Table 3. it is clear that final modulus of sliding is 38% of initial value ($K_{u,fin} = 0.38K_u$) for connection made of dowels. Ceccotti in [14] recommend push-out tests to obtain more realistic values of connection stiffness.

3.4.1 Corresponding normal and shear stress

Corresponding normal stresses as consequence of $M_{y,d,t}$ in $t = 0$ are given with equations (11) to (14) and they are represented in Fig. 8.

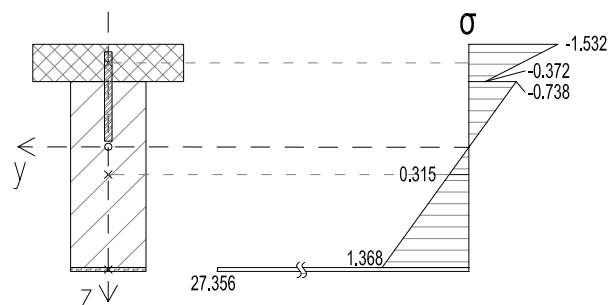


Fig. 8: Corresponding normal stresses (in kN/cm²).

Corresponding shear stresses as consequence of $V_{z,d,t}$ at $t = 0$ are given with equations (22) to (24) and they are represented in Fig. 9.

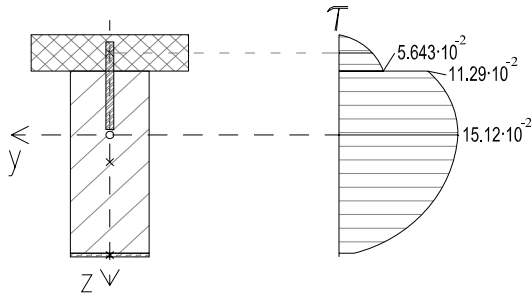


Fig. 9: Corresponding shear stresses (in kN/cm^2).

3.5 Numerical comparison between section with and without carbon strip

Relative comparison between load bearing capacity and bending stiffness of composite beam with and without carbon strip in function of variable intervals between dowels (material and geometrical properties are the same as in the upper example) is shown in following diagrams:

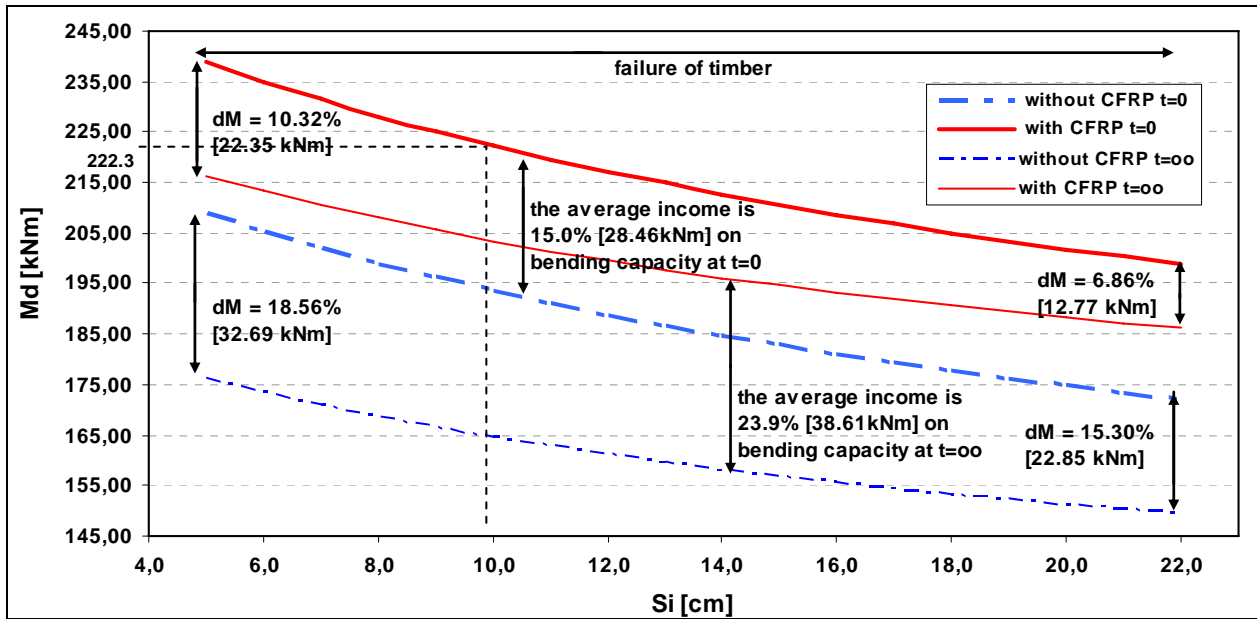


Fig. 10: Variability of bending load bearing capacity of composite cross section in function of spacing between dowels.

From diagrams in Fig 10. can be read initial ($t = 0$) bending bearing capacity (Md in function of dowel's spacing) of the structure with carbon strip which is 15% higher than the bearing capacity without it. Hence, the creep has big influence on rearrangement of stresses in section especially when section is composed from different creep depended materials. There can be also seen final ($t = \infty$) bending bearing capacity of the structure with carbon strip which is 24% higher than the bearing capacity without it.

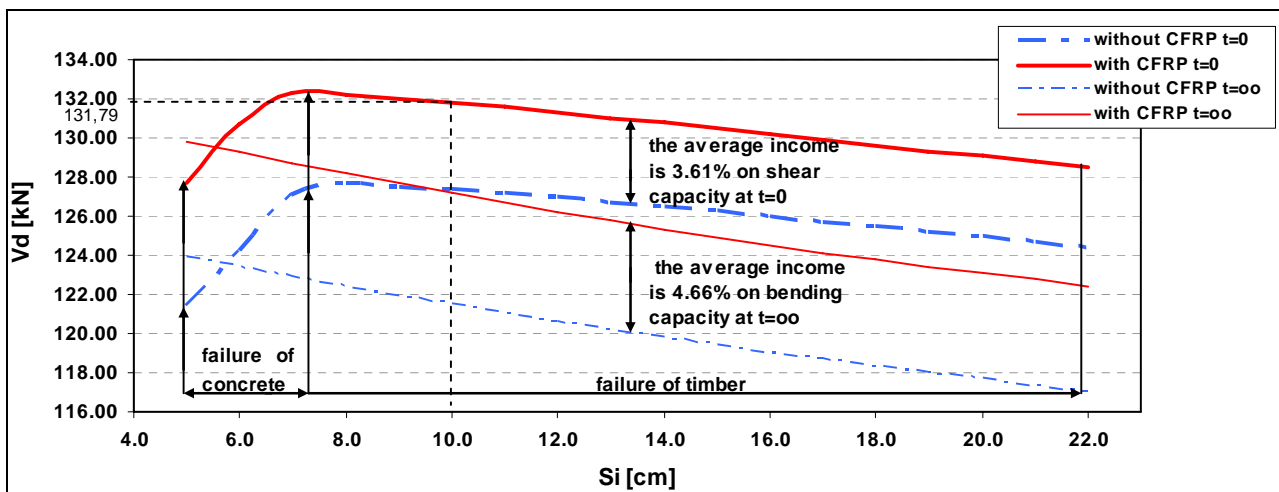


Fig. 11: Variability of shear load bearing capacity of composite cross section in function of spacing between dowels.

From diagrams in Fig 11. can be seen that carbon strip has practically no contribution to shear capacity of composite section and consecutively take no shear stress on it self. Therefore in practice we do not use it for shear capacity enlargement in such position.

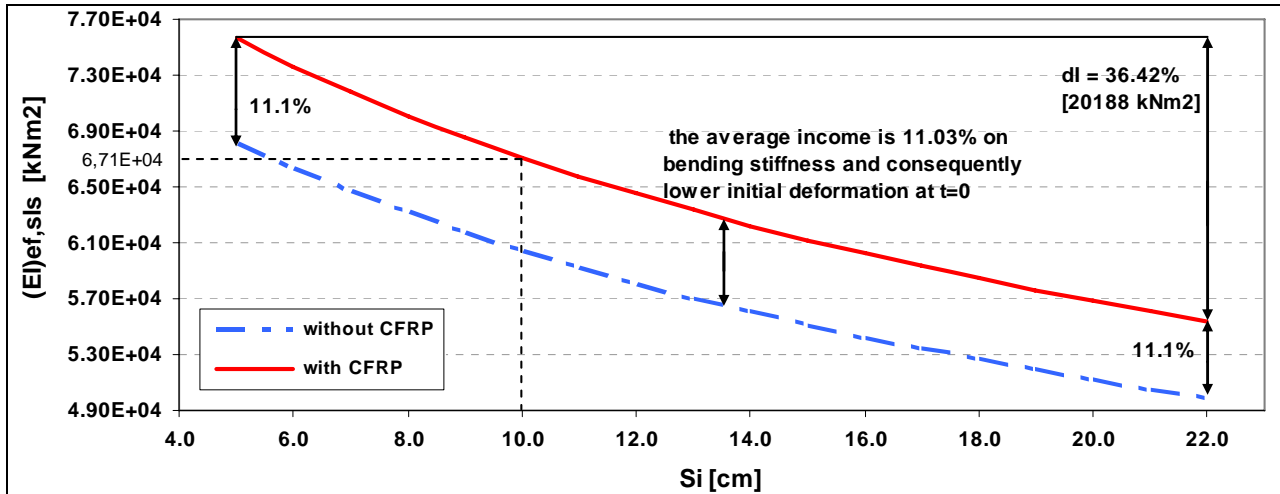


Fig. 12: Variability of initial bending stiffness of composite cross section in function of spacing between dowels.

Initial bending stiffness of strengthened section is 11.0% higher than un-strengthened section and final bending stiffness even higher and it is 17.5% (seen from diagrams in Fig 12. and Fig. 13).

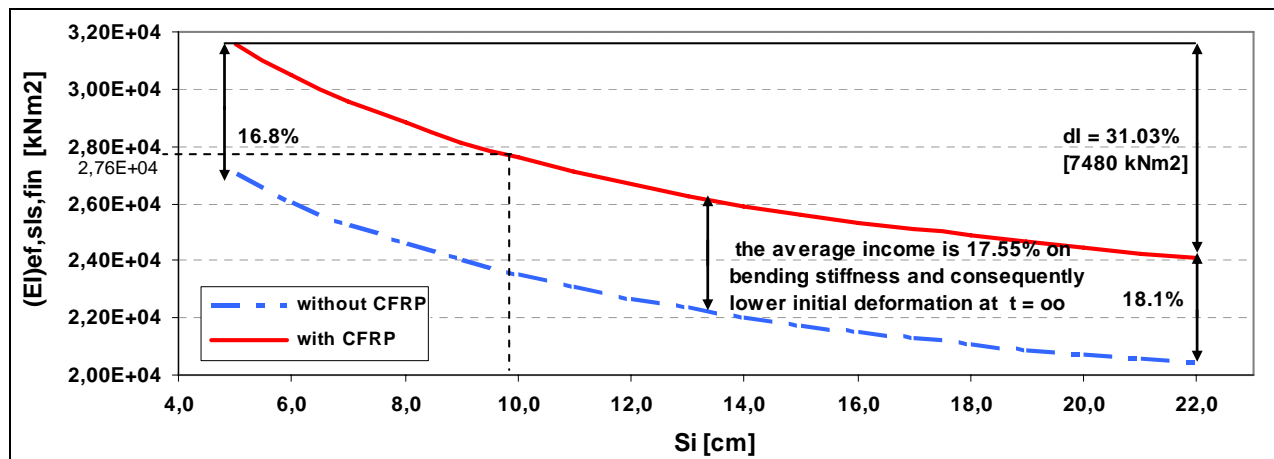


Fig. 13: Variability of final bending stiffness of composite cross section in function of spacing between dowels.

4 Conclusion

For presented composed sections in most cases (as well as in our study) the timber element is decisive at bottom tension side under ultimate bending loading. Because of that fact the strengthening with carbon strip is so important especially for final bending bearing capacity (because CFRP strip in comparison to timber and concrete do not creep). Presented study show an improvement of 15% on initial and 24% on final bending capacity, further at the same time is achieved improvement of 11% on initial and 17.5% on final bending stiffness. Furthermore the better combination of sub-components can significantly improve effects of

inclusion of CFRP strip. For example, higher bearing capacity and bending stiffness can be achieved with usage of carbon strip with higher Young's modulus because the timber ultimate bending strain is relatively low regarding to CFRP.

Under the influence of rearrangement of stresses in section shear stream on dowels is dropping with time which can be seen from Table 3. Consequently the initial loading is decisive for determination of fasteners load bearing capacity.

If in practise after such reinforcement (with CFRP strip) become decisive shear resistance of section than is suitably to use the carbon strip in position of stirrups

glued on web of timber beam similar like transverse steel reinforcement in steel reinforced concrete structures.

References:

- [1] M.Tajnik, *Comparison analysis of composite beam made of concrete and timber with and without carbon strip*, Faculty of Civil Engineering, University of Maribor, 2007.
- [2] M. Premrov, P. Dobrila, B.S. Bedenik, Analysis of timber-framed walls coated with CFRP strips strengthened fibre-plaster boards, *International Journal of Solids and Structures*, Vol.41, No. 24/25, pp. 7035–7048, 2004.
- [3] CEN/TC 250/SC5 N173, *Eurocode 5: Design of Timber Structures, Part 1-1 General rules and rules for buildings*, Final draft prEN 1995-1-1, Brussels, 2003.
- [4] prEN 1992-1-1, *Eurocode 2: Design of concrete structures, Part 1-1 General rules and rules for buildings*, Brussels, 2002.
- [5] ENV 1995-2, *Eurocode 5: Design of timber structures, Part 2 Bridges*, Brussels, 1997.
- [6] EN 1994-1-1, *Eurocode 4: Design of composite steel and concrete structures, Part 1-1 General rules and rules for buildings*, Brussels, 2004.
- [7] European Committee for Standardization, *EN 1194: Timber structures – Glued laminated timber – Strength classes and determination of characteristic values*, Brussels, 1999.
- [8] A. Frangi, M. Fontana, Elasto-Plastic Model for Timber-Concrete Composite Beams with Ductile Connection. *Structural Engineering International*, Vol.13, No.1, pp. 47-57, 2003.
- [9] K. Holschemacher, S. Klotz, D.Weibe, Application of Steel Fibre Reinforced Concrete for Timber-Concrete Composite Constructions, *Lacer*, No.7, pp. 161-170, 2002.
- [10] A. Ceccotti, *Holz-Brton-Verbundkonstruktionen, Step 2*, Bauteile konstruktionen details, Düsseldorf, pp. E13/1-11, 1995.
- [11] S. Kavaliauskas, A. Kvedaras, K. Gurkšnyš, Evaluation of long-term behaviour of composite timber-concrete structures according to EC, *Ukio technologinis ir ekonominis vystymas*, Vol.XI, No.4, pp. 292-296, 2005.
- [12] L. Bob, C. Bob, Researches regarding the behaviour of the composite wood-concrete floors, IABSE Conference Lahti 2001 - Innovative Wooden structures and Bridges, Vol.85, IABSE-AIPC-IVBH, pp. 531-536, 2001.
- [13] S. Takač, Đ. Matošević, P. Bogoičević, Rheological research of sliding modulus of the wood-concrete connection, IABSE Conference Lahti 2001 - Innovative Wooden structures and Bridges, Vol.85, IABSE-AIPC-IVBH, pp. 495-500, 2001.
- [14] A. Ceccotti, M. Fragiocomo, S. Giordano, Long-

term and collapse tests on a timber-concrete composite beam with glued-in connection, - *Springer Netherlands - Materials and Structures*, Vol.40, number 1, January, 2007.